Advances in the Science and Engineering of Casting Solidification
Edited by: Laurentiu Nastac, Baicheng Liu, Hasse Fredriksson, Jacques Lacaze, Chun-Pyo Hong, Adrian V. Catalina, Andreas Buhrig-Polaczek, Charles Monroe, Adrian S. Sabau, Roxana Elena Ligia Ruxanda, Alan Luo, Subhayu Sen, and Attila Diószegi
TMS (The Minerals, Metals & Materials Society), 2015

MODELING OF CASTING DEFECTS IN AN INTEGRATED COMPUTATIONAL MATERIALS ENGINEERING APPROACH

Adrian S. Sabau[1]
[1]Oak Ridge National Laboratory, Oak Ridge, Tennessee, 37831

Keywords: microporosity, simulation, modeling, nucleation, yield stress, hot tearing

Abstract

To accelerate the introduction of new cast alloys, the modeling and simulation of multiphysical phenomena needs to be considered in the design and optimization of mechanical properties of cast components. The required models related to casting defects, such as microporosity and hot tears, are reviewed. Three aluminum alloys are considered A356, 356 and 319. The data on calculated solidification shrinkage is presented and its effects on microporosity levels discussed. Examples are given for predicting microporosity defects and microstructure distribution for a plate casting. Models to predict fatigue life and yield stress are briefly highlighted here for the sake of completion and to illustrate how the length scales of the microstructure features as well as porosity defects are taken into account for modeling the mechanical properties. The data on casting defects, including microstructure features, is crucial for evaluating the final performance-related properties of the component.

INTRODUCTION

In castings, cavity defects can have regular, well-rounded shapes, or irregular, interdendritic shapes. For example, “hydrogen” microporosity consists of well-rounded and isolated voids while “shrinkage” microporosity and “hot-tear” defects are of irregular shape corresponding to the shape of the interdendritic region [1]. Over the last decades, industry has expanded the use of computer-aided engineering in reducing the manufacturing design and production cycle and cost, especially by implementing defect models into casting software. Integrated Computational Materials Engineering (ICME) has recently been established as a research protocol that combines theoretical analysis, design, and materials processing at the component level for materials design, including alloy development. In this study, the integration of casting defect modeling into an ICME framework is investigated.

For alloy design, it is desired to predict the resulting mechanical properties after heat treatment by taking into account casting defects and microstructure features (dendrite arm spacing, phases, amounts of phases, morphology, and lengthscales). In this context, for an ICME-based approach to the development of new cast alloys, the computational tools need to include the following models and data: (a) nucleation and growth models for defect during metal casting (e.g., microporosity, macroporosity, hot tearing), (b) process simulation models to obtain the size distribution within the casting of the microstructure length scales, phases, and defects, (c) microstructure/defects-to-mechanical property models to evaluate the resulting mechanical properties in as-cast condition, (d) precipitate nucleation and growth during heat treatment, and (e) microstructure/defects-to-mechanical property models to evaluate the resulting mechanical properties after heat treatment. In this study, the state-of-the art for microporosity defect

prediction, including the integration of data on porosity defects and microstructure features in an ICME-based approach, is reviewed.

In the last decade, truly coupled multi-physics software were developed specifically for metal casting by coupling most of the phenomena relevant to metal casting: fluid dynamics, stress evolution, diffusion, microstructure evolution, and defect formation/evolution. With the exception of several success stories in truly applying ICME-like methodologies [2-5], most ICME studies were about combined experimental-modeling of individual phenomena, such as grain growth, grain recrystallization, and prediction of stress-strain response with only a few presentations showing some actual "integrated" computational materials science and engineering results.

For alloy development studies, thermodynamics-based simulations, which can provide data on phases, phase stability, and amount of constituents, require short computational times and are widely used. However, as these thermodynamics-based simulations are geometry-less, a generic cooling rate expected during casting or a generic time-temperature schedule that includes not only the casting process but also the heat treatment step is as required at input. On the other hand, casting defects are not a material property but rather a result of the combined effect of fluid dynamics, diffusion, and microstructure evolution [6]. The availability of constitutive models for porosity defects and the much longer computational times required for process simulations poses a challenge to the ICME models.

REVIEW OF MODELS FOR MICROPOROSITY AND HOT TEARING

The amount of gas porosity, of regular shaped, isolated voids, can be very well predicted using models that include fluid dynamics, solidification, and gas segregation in molten alloys [7]. However, the prediction of irregular shaped porosity has been challenging. Recently, models have been proposed to formulate computational methodologies that can predict the occurrence of irregular shaped void defects, such as hot-tears and shrinkage porosity (Table I). In Table I, P_g is the gas pressure, P is the liquid metal pressure, P_c is the cavitation pressure of Al, and $P_S = 2\sigma/r$ is the pressure due to surface tension, σ, and f_g is the gas mass fraction. For the sake of completeness, it has to be mentioned that Sabau [8] proposed to estimate the degree of pore irregularity by the extent of pore growth after the cavitation pressure threshold has been reached.

Table III. Models for the onset of growth of irregular void defects [8].

Defect	*Fluid dynamics*	*Gas evolution*	*Stress*	*Porosity shape*	*Criteria and Reference*
microporosity	y	y	-	regular	$P_g > P + P_S$ [7]
shrinkage microporosity	y	y	-	*irregular*	$P_g > P + P_S$ and $P < P_c$ [1]
Hot tearing	y	-	y	irregular	$P < P_c$ [9]
Hot tearing	y	y	y	irregular	$P_g > P + P_S$ [10]
Microporosity and/or hot tearing	y	-	y	regular	$\partial f_g / \partial t > 0$ and/or $\sigma > \sigma_{\min}(d)$ [11]

One of the most important factors in microporosity growth is the pore curvature. Until recently the pore curvature was taken to be half of the secondary dendrite arm spacing. More accurate estimates for the cavity curvature, which is considered to be restricted by the solid dendrites, were developed by Pequet [12]. Recently, volatile elements were shown to affect the porosity formation in alloys since the nucleation and growth of pores in solidifying alloys was influenced by the partial vapor pressure of volatile solute elements [13]. However, these microporosity models predict only the average pore fraction at a given location in the casting, while the pore size distribution is needed for the prediction of fatigue resistance. Modeling the stochastic distribution of the pore size and density is a very active area of research [14-16]. Several submodels have been developed for the stochastic nucleation and diffusion-based growth of microporosity [17] by coupling Cellular Automata (CA) and finite element methods (FEM) in a similar manner as those developed solely for microstructure evolution [18, 19]. However, due to the complex phenomena involved, such as heterogeneous nucleation of microporosity and pore migration, no comprehensive model is yet available for microporosity shape prediction similar to the CAFE models for microstructure evolution [18, 19]. Direct numerical simulation CA-FE models for the prediction of microporosity defect distribution in entire shape castings are prohibitively computational intensive. Lee et al. [17] used physics-based correlations for predicting microporosity lengthscales in complex 319 Al alloy cast components. It has to be mentioned that these physics-based correlations, such as the one for the maximum pore length [17], were developed based on CA simulation results for a representative control volume for different process variables, including solidification time, hydrogen content, Cu content, and liquid pressure as opposed to empirically developed correlations that were used for decades with limited results when the casting shape was changed. However, only the proposed equation is available for the maximum pore length correlation in 319 Al alloy, as the actual parameters used in the correlation have not been published [17].

MICROSTRUCTURE COMPUTATIONAL RESULTS

Three alloys were considered in this study, as shown in Table II, in order to illustrate how microporosity depends on alloy composition in order to develop ICME-based practices for alloy design that take into account a realistic microstructure with intrinsic defects that lower their mechanical performance. Ni [%wt] is 0.029, 0.002, and 0.013; Pb[%wt] is 0.021, <0.001, and 0.007 for 319, A356, and 356, respectively, while Na, Sr, P, B, Ca, Sb were present at ppm levels. The thermodynamic simulations were conducted only for the as-cast condition, as the thermodynamic models of the microstructure evolution during heat treatment have not yet been implemented in ProCAST.

Table II. Composition of aluminum alloys considered [% wt].

Elem./ Alloy	Si	Cu	Fe	Mn	Zn	Ti	Cr	Sn
319	8.29	3.17	0.683	0.393	0.337	0.313	0.166	0.035
A356	7.32	0.002	0.1	0.044	0.402	0.005	0.156	<0.001
356	7.21	0.138	0.385	0.254	0.372	0.169	0.183	0.021

The typical microstructure for the alloys consisted of α-Al, Al_5FeSi (β- AlFeSi), Al_2Cu (AlCu-θ), eutectic Si phases and porosity, where the terminology used in the ProCAST and/or CompuTherm is indicated in parenthesis [20, 21]. The microstructure model in ProCAST was

used to conduct the thermodynamic simulations for the three alloys considered based on a back diffusion model for a constant cooling rate of 1 ^{o}C/s. The type of phases and their predicted amounts at the end of solidification for the three alloys considered are listed in Table III. The phase stability of precipitates is a very important factor in attaining adequate mechanical properties and the heat treatment effects on the as-cast microstructure need to be considered in further studies.

Table III. Phases and their calculated volumetric concentration [%] using the Al material database (Computherm) and microstructure module in ProCAST for the as-cast condition.

Phase/ Alloy	α-Al	*D-A4	Al_2Cu	$Al_{15}FeMn_3Si_2$	Al_5FeSi	$Al_5Cu_2Mg_8Si_6$	$Al_8FeMg_3Si_6$	Al_3Ti	Al_3Ni_1	Mg_2Si
319	84.90	6.53	2.9069	2.386	1.246	0.5445	-	0.376	0.039	-
A356	92.59	5.73	-	0.166	0.215	-	0.142	0.297	-	0.168
356	90.98	5.52	-	1.347	0.647	-	0.119	0.375	-	0.019

*Diamond-A4

EVALUATION OF SOLIDIFICATION SHRINKAGE

Using accurate material properties is paramount to the accuracy of process simulations. Through partnerships with thermodynamic database and software developers, the current-state-of the art metal casting software enables the evaluation of the following material properties: density in the liquid, mushy zone, and solid phase, thermal expansion, thermal conductivity, specific heat, viscosity of the molten metal, Young's modulus, and yield stress (YS). As an example of this emerging thermodynamic-based capability, results are presented in Figure 1 for the density. In order to illustrate the density variation in the latest stages of solidification, the density and temperature were shown in dimensionless form in Figure 1b. These data shows that there is significant variation in the shrinkage in the last stages of solidification among the three alloys considered. This last stage solidification shrinkage is very difficult to feed, as the liquid fraction is low, permeability becomes very low, resulting in large pressure drops in the mushy zone. Thus severe microporosity and hot tear defects are expected to occur, as discussed in the next section.

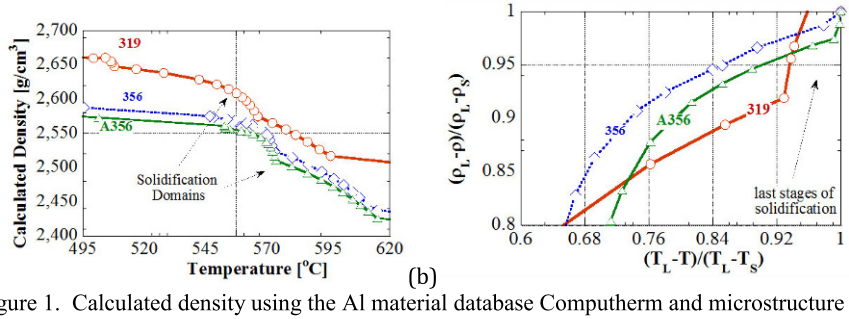

Figure 1. Calculated density using the Al material database Computherm and microstructure module in ProCAST for the alloys considered: (a) data (b) dimensionless data.

CASTING SIMULATION RESULTS

Numerical simulation results are presented in this section for a plate casting with cast iron chills (Sabau and Viswanathan, 2002). The mesh used in the computations is shown in Figure 2. The plate dimensions are 14 x 22.9 x 3.2 cm. The top and bottom chill dimensions were nominally 20 x 15 x 2.5 cm. The end-chill dimensions were nominally 6 x 15 x 6 cm. All the plates were contained in sand molds with nominal dimensions of 59 x 29 x 15.5 cm, respectively. ProCAST software was used in this study for metal casting simulations [22]. For Al alloys considered in this study, the model of the nucleation of the primary dendritic grains is that presented by Rappaz et al. [23, 24] based on a distribution of solid nuclei with undercooling. The nucleation of the eutectic grains is based on the model introduced by Oldfield [25]. In Figure 3, the following microstructure variables are shown: (a) secondary dendrite arm spacing (SDAS), (b) eutectic grain radius (EGR), which is the radius of the eutectic grains that nucleate in between the dendrites of the primary phase, and (c) eutectic lamellar spacing (ELS), which is the average distance between the eutectic lamellae or rods. Excluding the end plate regions (approx. last 4 cm on either side), these microstructural length scales for SDAS, EGR and ELS are uniform through the plate length. Near the plate top surface and bottom surface, the microstructure length scales are different from the core region.

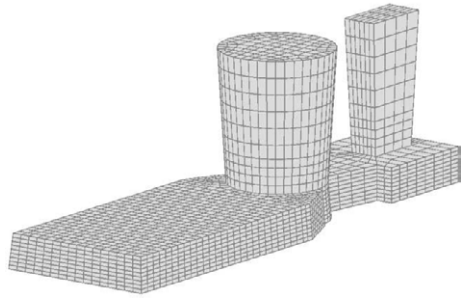

Figure 2. Finite element mesh used for metal casting simulations of a plate, including riser and sprue.

Numerical simulation results for microporosity, which were obtained with the advanced microporosity model available in ProCAST [12, 13], are shown for the three alloys in Figure 4a, b, and c (initial hydrogen content of 0.1cc/100g). The region with microporosity higher than 0.2% is referred in the remainder of this section as the high-microporosity region. For the A356 case (initial hydrogen content of 0.112cc/100g), the high-microporosity region is shown to appear slightly toward the plate end, extending from distances of 2.3 to 19.4 cm (from the plate end), while the experimental data presented in Sabau and Viswanathan [1] indicate that average porosity values larger than 0.2% covered a region from 3.9 to 13 cm (as measured from the plate end). Thus, the location of highest porosity region for A356 simulation is in good agreement with experimental data; however its predicted length is larger than that estimated from porosity measurements.

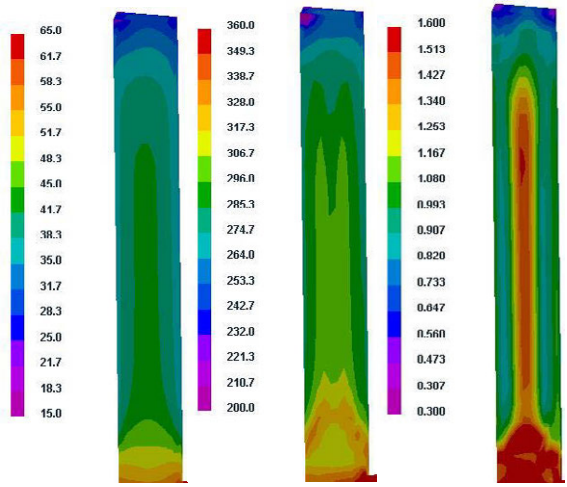

Figure 3. Computed distribution within the chilled-sand cast A356 casting in the vertical cross-section of the plate (plate end is on the top) for the: (a) SDAS [μm], (b) eutectic grain radius [μm], and (c) eutectic lamellar spacing [μm].

These results for the position of the region with microporosity higher than 0.2% are summarized for the alloys considered in Figure 5b. For the A356 case with initial hydrogen content of 0.1cc/100g, the high-microporosity region is shown to appear slightly toward the plate end, extending from distances of 2.6 to 18.1 cm. For the 356 case, the maximum porosity is higher than that for A356 and its distribution is quite different, e.g., the core along the centerline exhibits a lower porosity region than those above and below it. The predicted high-porosity region for 356 is located, with respect to the plate end, from 7.3 to 16.6 cm. For the 319, the length of the high-porosity region and the maximum microporosity value were found to be the largest among the three alloys considered. This is somehow expected, as shrinkage demand in the last stages of solidification is highest for 319, as shown in Figure 1b. The calculated high-porosity region for 319 alloy was found to be located at distances of 1.4 to 19.6 cm (with respect to the plate end).

The minimum pressure in the interdendritic liquid is shown in Figure 4 d, e, and f. Based on models presented in Pequet et al. (2002); Couturier and Rappaz (2006) the negative pressures in the liquid are allowed, as long as $P_g = P + P_S \geq 0$. On the other hand, the pressure levels below the cavitation pressure of Al were associated with severe shrinkage regions, regions in which the microporosity is irregular in shape [1, 8]. Thus, the negative pressure values, as the cavitation pressure of Al is very small at the solidus temperature, can be used as an indicator of a change in the porosity morphology, from rounded porosity defects to irregular-shaped porosity defects. This severe shrinkage region is thus expected to extend from 2 to 17.6 cm, 5.4 to 18 cm, and 1.5 to 18.5 cm for A356, 356 and 319 alloys, respectively, with respect to the plate end.

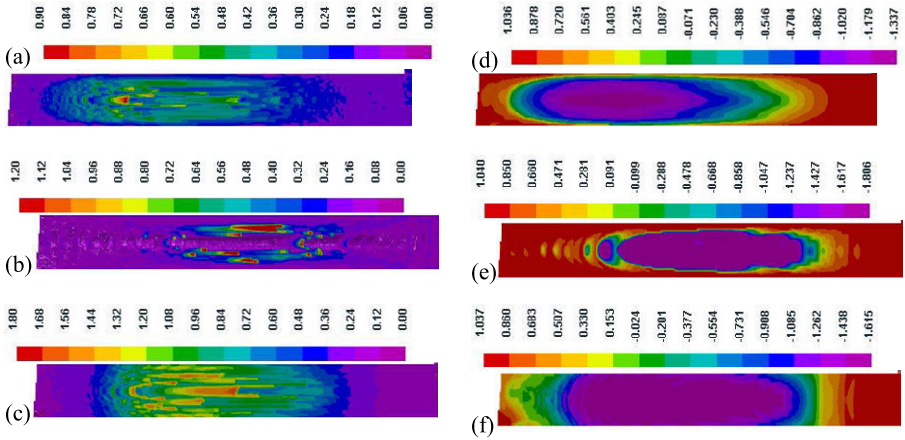

Figure 4. Microporosity prediction results for (a) A356, (b) 356, (c) 319. Corresponding minimum pressure in the liquid (d) A356, (e) 356, (f) 319 (plate end is located at the left-hand side).

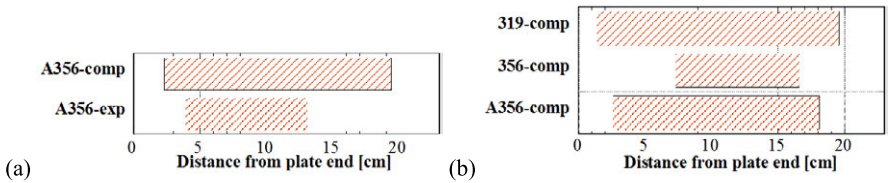

Figure 5. Location of the region with microporosity larger than 0.2%: (a) experimental and computed results for A356 alloy at an initial hydrogen content of 0.112cc/100g, and (b) for the alloys considered and an initial hydrogen content of 0.1cc/100g.

MICROSTRUCTURE/DEFECTS-TO-MECHANICAL PROPERTY MODELS

One of the most challenging steps in ICME-like approaches is the prediction of mechanical properties based on the calculated or measured distribution of both microstructure and void defects. Fatigue life and yield stress are briefly highlighted here for the sake of completeness and to illustrate how the length scales of the microstructure features as well as porosity defects are taken into account for modeling the mechanical properties. The following microstructure features can significantly affect the fatigue crack initiation and its growth behavior: SDAS, size and distribution of silicon particles, fracture resistance of silicon, strength of interface between silicon and aluminum matrix, intermetallics, and porosity [26]. A microstructure based-fatigue model is desired in order to be able to account for the effect of these stress concentrators [27].

A Hall-Petch type equation is used to describe the strength variation due to change in SDAS, λ_2, for the primary dendrite phase and the eutectic laminar spacing, λ, for the eutectic phase. The as cast yield strength can be written, as (Guo and Scott, 2002):

$$\sigma_c = f_p(\sigma_o + \frac{k_p}{\lambda_2^{1/2}}) + f_e \frac{k_e}{\lambda^{1/2}} + \sigma_P \quad (1)$$

where f_p and f_e are volume fraction of primary and eutectic phases respectively. σ_o, k_p, and k_e are solid solution stress and the Hall-Petch coefficient for the primary phase and eutectic phase. The third term accounts for the strengthening due to precipitates that nucleate and grow during the heat treatment. Unfortunately, the current-state-of the art metal casting software allows for the calculation of the yield stress within the entire casting only at room temperature for the as-cast condition based on the final microstructure distribution. To date, the heat treatment microstructure has to be simulated at discrete locations in the casting using stand-alone thermodynamic software based on actual cooling/heating/quenching curves that were obtained from a metal process casting simulation. This is due in large part to the fact that models for the microstructure evolution during heat treatment are not as mature as those for microstructure evolution during casting solidification. Microporosity, which obviously decreases mechanical properties, is not considered in the above equation.

DISCUSSIONS AND CONCLUSIONS

The simulation of the metal casting processes can be conducted very effectively using the thermophysical and thermo-mechanical properties calculated from thermodynamic considerations as input. Casting defects are not a material property but rather a result of the combined effect of fluid dynamics, diffusion, and microstructure evolution. Data on casting defects, including microstructure features, is essential for evaluating the final performance-related properties of the cast component. Approaches for the prediction of irregular-shaped porosity have been reviewed. To date, models for microporosity defect prediction are limited to the volumetric fraction of porosity. Models for the prediction of the stochastic variables that describe the distribution of the pore size and density are being developed and not yet available to the community at large.

The spatial distribution of the as-cast microstructure length-scales can be accurately predicted. To date, the distribution of the amount and morphology of strengthening precipitates following a *heat treatment* cannot be simulated in the entire casting. Microstructure-to-property models that would take into account the distribution within the component of the as-heat-treated microstructure and casting defects are being developed to predict both the yield stress at operating temperatures and in-service overall performance of the component.

ACKNOWLEDGEMENTS

This work was performed under a Cooperative Research and Development Agreement (CRADA) with the Nemak Inc., and Chrysler Co. for the project "High Performance Cast Aluminum Alloys for Next Generation Passenger Vehicle Engines." The author would also like to thank Amit Shyam for reviewing the paper and Andres Rodriguez of Nemak Inc. Research sponsored by the U. S. Department of Energy, Office of Energy Efficiency and Renewable Energy, Vehicle Technologies Office, as part of the Propulsion Materials Program under contract

DE-AC05-00OR22725 with UT-Battelle, LLC. Part of this research was conducted through the Oak Ridge National Laboratory's High Temperature Materials Laboratory User Program, which is sponsored by the U. S. Department of Energy, Office of Energy Efficiency and Renewable Energy, Vehicle Technologies Program.

REFERENCES

1. Sabau, A.S. and Viswanathan, S, "Microporosity Prediction in Aluminum Alloy Castings," Metallurgical and Materials Transactions B, 2002, Vol. 33B, pp. 243-255.
2. NRC, 2008, "Integrated Computational Materials Engineering (ICME): A Transformational Discipline for Improved Competitiveness and National Security", Committee on Integrated Computational Materials Engineering, National Research Council.
3. Miller, L.K.; "Simulation-Based Engineering for Industrial Competitive Advantage," Computing in Science & Engineering, vol.12, no.3, pp.14-21, 2010.
4. Allison J, Backman D, Christodoulou L, 2006, Integrated computational materials engineering: A new paradigm for the global materials profession, JOM, Vol. 58, pp. 25-27.
5. Allison, J., Mei Li, C. Wolverton, and Xu Ming Su, 2006, Virtual Aluminum Castings: An Industrial Application of ICME. JOM, Vol. 58, pp. 28-35.
6. A.S. Sabau, W.D. Porter, S. Roy, and A. Shyam, Process Simulation Role in the Development of New Alloys Based On An Integrated Computational Materials Engineering Approach, paper IMECE2014-37982, Proceedings of the ASME 2014 Int. Mech. Eng. Congress & Exposition IMECE2014, Nov. 14-20, 2014, Montreal, Quebec, Canada.
7. K. Kubo and R. D. Pehlke: *Metall. Trans. B*, 1985, vol. 16B, pp. 359-66.
8. Sabau, A.S. Predicting Interdendritic Cavity Defects during Casting Solidification, JOM, 2004, Vol. 56, pp. 54-56.
9. Rappaz M. Drezet, JM; Gremaud, M, "A new hot-tearing criterion," *Metall. Mater. Trans. A*., Vol. 30, (1999), pp. 449-455.
10. J. F. Grandfield, C. J. Davidson, and J. A. Taylor, "Application of a New Hot Tearing Analysis in Horizontal Direct-Chill Cast Magnesium Alloy AZ91," Light Metals, (131st TMS Annual Meeting and Exhibition), Seattle (USA), 11-15 February 2001, pp. 207-213.
11. Suyitno, W.H. Kool, and L. Katgerman, *Mater. Sci. Forum*, Vols. 396-402 (2002), pp. 179-184.
12. C. Pequet, M. Gremaud, and M. Rappaz, "Modeling of Microporosity, Macroporosity, and Pipe-shrinkage Formation During the Solidification of Alloys Using a Mushy-zone Refinement Method: Applications to Aluminum Alloys," *Metall. Mater. Trans. A*., Vol. 33, (2002) pp. 2095-2106.
13. G. Couturier and M. Rappaz, Modelling and Simulation in Materials Science and Engineering, Vol. 14, pp. 253, 2006.
14. P.D. Lee, A. Chirazi, D. See, Modeling microporosity in aluminum±silicon alloys: a review, Journal of Light Metals 1 (2001), pp. 15-30.

15. R.C. Atwood, P.D. Lee, Simulation of the three-dimensional morphology of solidification porosity in an aluminium–silicon alloy, Acta Materialia, Vol. 51, pp. 544–5466, 2003.
16. Wang, J.; Li, M.; Allison, J.; and Lee, P.D, Multiscale modeling of the influence of Fe content in a Al-Si-Cu alloy on the size distribution of intermetallic phases and micropores, Journal of Applied Physics, Vol. 107, Article No. 061804, 2010.
17. P. D. Lee, A. Chirazi, R. C. Atwood, and W. Wang, Multiscale modelling of solidification microstructures, including microsegregation and microporosity, in an Al–Si–Cu alloy, Mater. Sci. Eng., A 365, p. 57, 2004.
18. Ch.-A. Gandin and M. Rappaz, *Acta Metall. Mater.,* 42 (1994), pp. 2233–2246.
19. Ch.-A. Gandin, J.-L. Desbiolles, M. Rappaz and Ph. Thevoz, *Metall. Mater. Trans.*, 30A (1999), pp. 3153–3165.
20. J. Guo and M. T. Samonds T. "Property prediction with coupled macro-micromodeling and computational thermodynamics," Proc. of MCSP6, Taiwan: Kaohsiung, 2004, pp. 157-164.
21. J. Guo and M. T. Samonds, Alloy Thermal Physical Property Prediction Coupled Computational Thermodynamics with Back Diffusion Consideration, Journal of Phase Equilibria and Diffusion, 2007, Vol. 28, pp. 58-63.
22. J. Guo and M. T. Samonds, Modeling of alloy casting solidification, Journal of Metals, Vol. 63, 2011, pp. 19-28.
23. M. Rappaz and Ph. Thevoz, *Acta Metall.*, 1987, vol. 35, pp. 1487–97.
24. M. Rappaz and Ph. Thevoz, *Acta Metall.*, 1987, vol. 35, pp. 2929–33.
25. W. Oldfield, ASM Transactions, 1996, Vol. 59, pp. 945-61.
26. Ye H., An overview of the development of Al-Si-Alloy based material for engine applications, Journal of Materials Engineering and Performance, 2003, Volume 12, pp. 288-297.
27. D.L McDowell, K Gall, M.F Horstemeyer, J Fan, Microstructure-based fatigue modeling of cast A356-T6 alloy, Engineering Fracture Mechanics, Vol. 70, 2003, pp. 49–80.